

Electrical and optical properties of p-type ZnO

This article has been downloaded from IOPscience. Please scroll down to see the full text article.

2005 Semicond. Sci. Technol. 20 S55

(<http://iopscience.iop.org/0268-1242/20/4/007>)

View [the table of contents for this issue](#), or go to the [journal homepage](#) for more

Download details:

IP Address: 138.253.19.98

The article was downloaded on 04/01/2013 at 16:25

Please note that [terms and conditions apply](#).

Electrical and optical properties of p-type ZnO

David C Look

Semiconductor Research Center, Wright State University, Dayton, OH 45435, USA

Received 27 September 2004

Published 15 March 2005

Online at stacks.iop.org/SST/20/S55

Abstract

ZnO has ideal qualities for bright, efficient UV light emitting diodes and laser diodes, based on p–n junctions. However, while high quality n-type ZnO has been available for many years, the development of good p-type material is a much more recent phenomenon. The most successful acceptor dopants have been the group V elements, N, P and As; N substitutes on the O site, but the exact structures of the P and As acceptors have not yet been established. Resistivities as low as $0.4 \Omega \text{ cm}$ have been measured, and some UV heterojunction and homojunction LEDs have been fabricated. Optical fingerprints of p-type ZnO often include a photoluminescence line at 3.31 eV, and strong donor-bound exciton lines at 3.357 and 3.367 eV, both of which are well known from previous studies of n-type ZnO.

Introduction

ZnO has long been proposed as a strong candidate for electronic [1] and UV/photonic [2, 3] applications. The driving force for the photonic applications is the stability of the ZnO free exciton, which has a binding energy of 60 meV in bulk material, and an even higher value in confined structures. This binding energy is more than twice that of the GaN free exciton, a significant comparison considering that the GaN material system is the one presently used in most semiconductor-based blue and UV emitters. ZnO also has many other advantages, including the availability of large-area native substrates, amenability to low-temperature growth and wet chemical etching and high radiation resistance. But ZnO also has one major disadvantage, the lack of a reliable technology for producing p-type material. Fortunately, in recent years, this situation has improved, and now several groups have reported p-type ZnO [4–29], and a few have even produced light-emitting p–n junctions (for detailed discussions, see [30, 31]). However, most of the basic aspects of p-type ZnO are still not well understood, and that lack of knowledge will impede further progress. In this work, we will review what is known about the electrical and optical properties of p-type ZnO, in particular, what has been learned from temperature-dependent Hall-effect (T-Hall) and photoluminescence (PL) measurements, respectively. We will discuss T-Hall theory and experiments in some detail, because Hall voltages are small in p-type ZnO, and consequently they must be measured and analysed with great care. Indeed, there

is still much scepticism regarding the very existence, or at least the stability, of p-type ZnO, probably because of the history of unsuccessful, questionable and unverifiable attempts to produce it. It is hoped that this review will dispel some of that negative opinion and provide a basis for further progress in this field.

Hall-effect theory

The basic equations for Hall-effect analysis, allowing for the energy dependence of the electrons, are as follows [32]:

$$j_x = \frac{ne^2\langle\tau\rangle}{m^*} E_x \equiv -ne\mu_c E_x \quad (1)$$

$$R_H = \frac{E_y}{j_x B} = -\frac{1}{ne} \frac{\langle\tau^2\rangle}{\langle\tau\rangle^2} = -\frac{r}{ne} \quad (2)$$

where electric E and magnetic B fields are imposed in the x and z directions, respectively, and

$$\begin{aligned} \langle\tau^n(E)\rangle &= \frac{\int_0^\infty \tau^n(E) E^{3/2} \frac{\partial f_0}{\partial E} dE}{\int_0^\infty E^{3/2} \frac{\partial f_0}{\partial E} dE} \\ &\rightarrow \frac{\int_0^\infty \tau^n(E) E^{3/2} e^{-E/kT} dE}{\int_0^\infty E^{3/2} e^{-E/kT} dE} \end{aligned} \quad (3)$$

where the integration is over energy E . (Although these equations are written for electron current, they hold equally well for hole current with the simple transformation $n \rightarrow p$ and $e \rightarrow -e$.) This formulation is called the relaxation-time approximation (RTA) to the Boltzmann transport equation

(BTE). Here f_0 is the Fermi–Dirac distribution function and the second equality in equation (3) holds for non-degenerate electrons, i.e., those describable by Boltzmann statistics. The quantity $\mu_c = e\langle\tau\rangle/m^*$ is known as the ‘conductivity’ mobility, since the quantity $ne\mu_c$ is just the conductivity σ . We define the ‘Hall’ mobility as $\mu_H = R_H\sigma = r\mu_c$, and the ‘Hall’ concentration as $n_H = n/r = -1/eR_H$. Thus, a combined Hall-effect and conductivity measurement gives n_H and μ_H , although we would prefer to know n , not n_H ; fortunately, however, r is usually within 20% of unity, and is almost never as large as two. In any case, r can often be calculated or measured so that an accurate value of n can usually be determined.

The relaxation time, $\tau(E)$, depends upon how the electrons interact with the lattice vibrations as well as with extrinsic elements, such as charged impurities and defects. For example, acoustical-mode lattice vibrations scatter electrons through the deformation potential (τ_{ac}) and piezoelectric potential (τ_{pe}); optical-mode vibrations through the polar potential (τ_{po}); ionized impurities and defects through the screened Coulomb potential (τ_{ii}); and charged dislocations, also through the Coulomb potential (τ_{dis}). The strengths of these various scattering mechanisms depend upon certain lattice parameters, such as dielectric constants and deformation potentials, and extrinsic factors, such as donor, acceptor and dislocation concentrations N_D , N_A and N_{dis} , respectively. The total momentum scattering rate, or inverse relaxation time, is

$$\tau^{-1}(E) = \tau_{ac}^{-1}(E) + \tau_{pe}^{-1}(E) + \tau_{po}^{-1}(E) + \tau_{ii}^{-1}(E) + \tau_{dis}^{-1}(E) \quad (4)$$

and this expression is then used to determine $\langle\tau^n(E)\rangle$ via equation (3), and thence, $\mu_H = e\langle\tau^2\rangle/m^*\langle\tau\rangle$. Formulae for τ_{ac} , τ_{pe} , τ_{po} , τ_{ii} and τ_{dis} , can be found in the literature [32, 33], but τ_{ii} , and τ_{dis} will be discussed further here. For ionized impurity (or defect) scattering, in a non-degenerate, n-type material:

$$\tau_{ii}(E) = \frac{2^{9/2}\pi\epsilon_0^2(m^*)^{1/2}E^{3/2}}{e^4(2N_A + n)[\ln(1+y) - y/(1+y)]} \quad (5)$$

where $y = 8\epsilon_0 m^* k T E / \hbar^2 e^2 n$. Here, ϵ_0 is the low-frequency (static) dielectric constant, k is Boltzmann’s constant and \hbar is Planck’s constant divided by 2π . (If the sample is p-type, let $(2N_A + n) \rightarrow (2N_D + p)$).

Dislocation scattering in semiconductor materials is often ignored, because it becomes significant only for dislocation densities $N_{dis} > 10^8 \text{ cm}^{-2}$ (note that this is an *areal*, not *volume*, density). Such high densities are rare in most semiconductor devices, such as those fabricated from Si or GaAs, but are indeed quite common in devices based on ZnO or other materials which involve mismatched substrates. In ZnO grown on Al_2O_3 (sapphire), vertical threading dislocations, typically of concentration 10^{10} cm^{-2} or higher, emanate from the interface up to the surface, and horizontally moving electrons or holes experience a scattering characterized by [33]

$$\tau_{dis}(E) = \frac{\hbar^3 \epsilon_0^2 c^2}{N_{dis} m^* e^4} \frac{(1 + 8m^* \lambda^2 E)^{3/2}}{\lambda^4} \quad (6)$$

where $\lambda = (\epsilon_0 k T / e^2 n)^{1/2}$. For the best ZnO/ Al_2O_3 layers, $N_{dis} \approx 10^8 \text{ cm}^{-2}$; this value of N_{dis} would drop the 300 K Hall mobility by only a minor amount. However, for a sample with

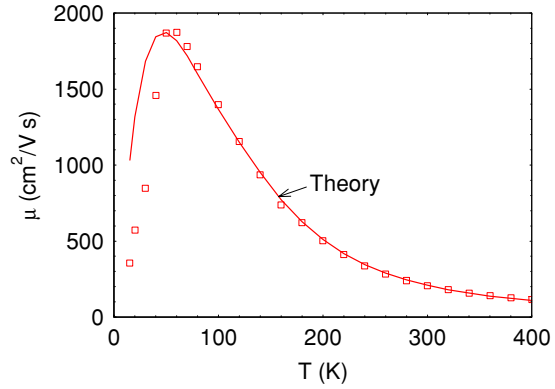


Figure 1. Temperature dependence of electron mobility for bulk, undoped, n-type ZnO, grown from the vapour phase. The solid line is a least-squares fit to the data.

the usual concentration of dislocations found in ZnO/ Al_2O_3 , about 10^{10} cm^{-2} , the mobility would drop to less than $100 \text{ cm}^2 (\text{V s})^{-1}$, a typical value found in many epitaxial ZnO layers.

The fitting of μ_H versus T data, described above, should be carried out in conjunction with the fitting of n versus T , which is derived from the charge-balance equation (CBE):

$$n + N_A = \sum_i \frac{N_{Di}}{1 + n/\phi_{Di}} \quad (7)$$

where the subscript i denotes a particular donor and where

$$\phi_{Di} = \frac{g_{0i}}{g_{1i}} e^{\frac{\alpha_{Di}}{k}} N'_C T^{3/2} e^{-\frac{E_{D0i}}{kT}}. \quad (8)$$

For each donor, g_0/g_1 is a degeneracy factor, $N'_C = 2(2\pi m_n^* k)^{3/2}/h^3$ is the effective conduction-band density of states at 1 K, h is Planck’s constant, E_D is the donor energy and E_{D0} and α_D are defined by $E_D = E_{D0} - \alpha_D T$. Equation (7) describes the simplest type of charge balance, in which each of the one or more donors has only one charge-state transition within a few kT of the Fermi energy. An example of such a donor is Ga on a Zn site in ZnO. If there are double or triple donors, or more than one acceptor, proper variations of equation (7) can be found in the literature [32].

We will illustrate the T-Hall methodology with analysis of a bulk, n-type ZnO sample [34], of square shape and grown by the seeded vapour transport method. Small indium dots were soldered on the corners to provide ohmic contacts, and the Hall measurements were carried out in an automated apparatus, a LakeShore Model 7507. The temperature dependences of μ_H and n are shown in figures 1 and 2, respectively. The following parameters were taken from the literature: piezoelectric coupling coefficient $P = 0.21$; low-frequency dielectric constant $\epsilon_0 = 8.12(8.8542 \times 10^{-12}) \text{ F m}^{-1}$; high-frequency dielectric constant $\epsilon_\infty = 3.72(8.8542 \times 10^{-12}) \text{ F m}^{-1}$; polar-optical temperature $T_{po} = 837 \text{ K}$; effective mass $m^* = 0.318(9.1095 \times 10^{-31}) \text{ kg}$; mass density $\rho_d = 6.10 \times 10^3 \text{ kg m}^{-3}$; speed of sound $s = 6.59 \times 10^3 \text{ m s}^{-1}$; unoccupied-state degeneracy $g_0 = 1$; occupied-state degeneracy $g_1 = 2$; $\alpha_D = 0$; and $N'_C = 8.66 \times 10^{20} \text{ m}^{-3}$. The best value for deformation potential E_1 was found to be $15 \text{ eV} = 2.4 \times 10^{-18} \text{ J}$, although 3.8 eV is given by one literature source. The fitted parameters are: $N_{D1} = 9 \times 10^{15} \text{ cm}^{-3}$, $E_{D1} = 31 \text{ meV}$,

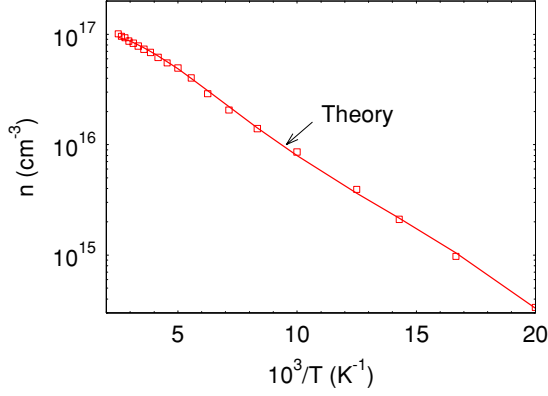


Figure 2. Arrhenius plot of electron concentration for bulk, undoped, n-type ZnO. The solid line is a least squares fit to the data.

$N_{D2} = 1.0 \times 10^{17} \text{ cm}^{-3}$, $E_{D2} = 61 \text{ meV}$ and $N_A = 2 \times 10^{15} \text{ cm}^{-3}$. These values of N_{D1} , N_{D2} and N_A show that good purity can be achieved in present-day ZnO.

T-Hall analysis in p-type ZnO

For a p-type sample, the simple CBE becomes

$$p + N_D = \sum_i \frac{N_{Ai}}{1 + n/\phi_{Ai}} \quad (9)$$

where $N'_V = 2(2\pi m_p^* k)^{3/2}/h^3$, $\phi_A = (g_1/g_0) N'_V \exp(\alpha_A/kT) \exp(-E_{A0}/kT)$ and $E_A = E_{A0} - \alpha_A T$, for each acceptor. Note that ϕ_A has the term ' g_1/g_0 ', which is inverted from the first term in equation (8) because the degeneracies still refer to electrons, not holes. From equation (9), it can be shown that the hole concentration in a nondegenerate, single-donor/single-acceptor model, will be given by [32]

$$p = \frac{1}{2}(\phi_A + N_D) \left\{ \left[1 + \frac{4\phi_A(N_A - N_D)}{(\phi_A + N_D)^2} \right]^{1/2} - 1 \right\} \quad (10)$$

where the various symbols were defined earlier. For N, P, As or Sb on an O site, we would expect that $g_{A0} = 4$ and $g_{A1} = 1$. If we assume an effective hole mass of $m_p = 0.64m_0$, then $N'_V = 2.47 \times 10^{15} \text{ cm}^{-3} \text{ K}^{-3/2}$. (This value of mass is a rough estimate based on a hydrogenic acceptor energy of 135 meV, which comes from the data of figure 3 extrapolated to low acceptor concentration by means of a screening analysis.) However, more accurate determinations of the effective hole mass will undoubtedly be available in future works.

Multicarrier effects and determination of type

Thin films are likely to be inhomogeneous with depth, especially if they are grown on a lattice mismatched substrate. Moreover, there are situations that may arise in which both holes and electrons are present, especially in a sample that has been exposed to strong UV light. For example, in a p-type ZnO sample, with bands bending downward at the surface, excited electrons may accumulate near the surface, and produce an opposing Hall voltage. In that case, we need to consider generalizations of the single-carrier model presented above.

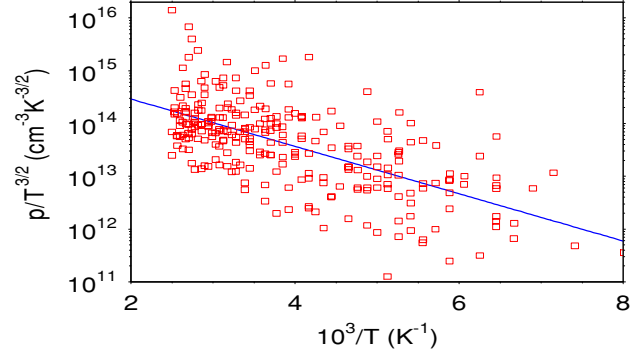


Figure 3. Arrhenius plot of $p/T^{3/2}$ for N-doped, p-type ZnO, grown by MBE on the Zn face (0001) of a bulk ZnO substrate. The solid line is a least-squares fit to the data.

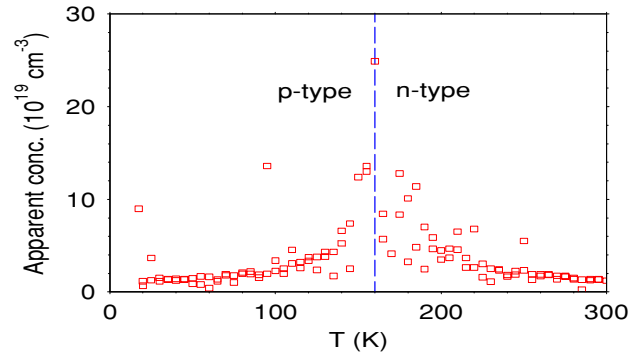


Figure 4. Temperature dependence of the apparent concentration in a P-doped, p-type ZnO layer after brief exposure to UV light at 20 K. The structure was: 0.5 μm thick p-type ZnO/1 μm thick SI ZnO/ Al_2O_3 .

If n , μ_n , p and μ_p vary with depth (z), then the measured quantities become

$$\sigma_{\text{sq}} = \int_0^d \sigma(z) dz = e \int_0^d [p(z)\mu_p(z) + n(z)\mu_n(z)] dz \quad (11)$$

$$R_{\text{Hsq}}\sigma_{\text{sq}}^2 = e \int_0^d [p(z)\mu_p^2(z) - n(z)\mu_n^2(z)] dz \quad (12)$$

where d is the sample thickness and where the subscript 'sq' denotes a sheet (areal) quantity (cm^{-2}) rather than a volume quantity (cm^{-3}). From equation (12), clearly R_{Hsq} can be negative (n-type) or positive (p-type), depending upon the integral of $p(z)\mu_p^2(z) - n(z)\mu_n^2(z)$. An example of this phenomenon is given in figure 4, in which UV light exposure has evidently produced a persistent n-type region, which dominates the p-type bulk region at high temperatures but not at low temperatures [31]. Note that the *simultaneous* existence of electrons and holes *in the same region* is unlikely in such a wide bandgap semiconductor. Thus, the data in figure 4 can best be explained by a competition between the holes in the bulk and UV-excited electrons forced to stay near the surface by the downward band bending.

Although the Hall-effect determination of type, based on the sign of $(p\mu_p^2 - n\mu_n^2)$, is widely employed, there are also other methods which may be more useful in certain situations. One such method makes use of the Seebeck effect,

which is realized by imposing a temperature gradient on the sample, and which will give a p-type response if $p\mu_p > n\mu_n$ [32]. This method is very simple, and qualitative results may be obtained by placing two voltage probes on the sample and a soldering iron near one of them. However, it is much more difficult to obtain quantitative information by this technique. Another method makes use of the Schottky-barrier-capacitance behaviour in the presence of an applied surface voltage. If a negative voltage causes a decrease in capacitance, then the material is n-type, and vice versa [35]. Although this technique, like the Seebeck technique, is quite convenient, it does require a Schottky barrier, and also samples only the material near the surface.

Returning to the Hall-effect, we consider two common problems often encountered when investigating p-type ZnO. Both of these problems arise from the small magnitude of the Hall field E_y , and can lead to false results, or at least destroy confidence in legitimate results. Indeed, from equations (1) and (2), $E_y = \mu BE_x$, and since $\mu \leq 1 \text{ cm}^2 (\text{V s})^{-1}$, E_y will be only about $10^{-4} E_x$, if $B \sim 1 \text{ T}$. This issue is further exacerbated by being forced to deal with noisy ohmic contacts in this early stage of p-type ZnO technology, although progress is being made [36]. Averaging over current and magnetic-field polarities, and the various van der Pauw configurations, requires a set of eight different measurements to get a single result, and a large noise spike during only one of these measurements can lead to a large error in the final result, even making the sample appear to be n-type. An example of hole concentration as a function of temperature is given in figure 3, and the high noise level is very apparent. Some of the measurements in this particular case were even n-type, as would be expected from such a large scatter. However, in spite of the large noise levels, a reasonable least-squares fit to equation (10) can be obtained, and the derived activation energy is about 90 meV [31]. A simple screening model then suggests that the energy at infinite acceptor dilution is about 135 meV, although this number is very approximate.

Besides high noise levels, a second problem encountered with measurements of p-type ZnO is persistent photoconductivity (PPC). If UV light impinges on the sample, electrons and holes are created, and sometimes the holes can become trapped, making them unavailable for recombination after the light is turned off. Since the electron mobility is much higher than the hole mobility, the nonequilibrium (persistent) electrons will turn the Hall voltage negative (n-type) if $n\mu_n^2 > p\mu_p^2$. This is indeed the case for the sample represented in figure 3, after it has been exposed to strong light, and it is probably also true for some of the other samples discussed in the literature that have been dismissed as ‘unstable’. Even the UV content in normal room light is sometimes enough to switch a weakly p-type sample to n-type.

To illustrate the PPC phenomenon, we consider the following structure, grown by the sputtering method: top layer, $0.5 \mu\text{m}$ thick, P-doped; buffer layer, $1.0 \mu\text{m}$ thick, undoped; substrate, Al_2O_3 . Note that this structure consists only of ZnO and Al_2O_3 , and since the latter is an insulator, any p-type conduction must be associated with the ZnO. Similar material was shown to be p-type and stable, in the dark, by those who developed it [19], and it has been confirmed in other laboratories, including our own. However, if the sample

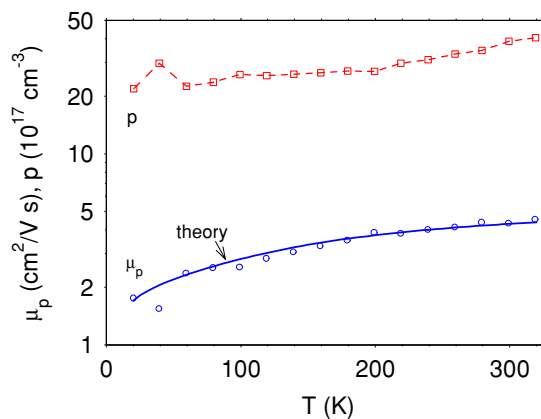


Figure 5. Temperature dependence (in the dark) of the hole concentration and mobility in an $0.5 \mu\text{m}$ thick, As-doped, p-type ZnO layer, grown on glass by sputtering. The solid line is a least-squares fit to the data.

is exposed to strong UV light, and then returned to a dark condition, it will remain p-type at the lowest temperatures but then become n-type at some higher value of temperature and remain n-type up to room temperature, as illustrated in figure 4. This is a reversible effect, meaning that the sample will return to p-type if the temperature is again lowered. If held at room temperature in the dark, the sample will remain n-type for many hours, but will gradually anneal back to p-type, and remain so at all temperatures. We tentatively interpret this effect in terms of donor states at the surface, which bend the bands downward. Exposure to UV light will then create electrons and holes, with the electrons being swept to the surface, and filling surface states, with energies close to that of the conduction band edge. As the temperature is raised, a certain fraction of these electrons become free, and provide a current in the plane parallel to the surface. This electron current eventually dominates the bulk hole current, and changes the sign of the Hall coefficient. At a high enough temperature, these non-equilibrium electrons are able to overcome the surface band bending, and recombine with holes in the bulk region, thus restoring the sample to p-type at all temperatures. Further details of this interesting phenomenon will be reported separately [37]; however, the existence of a transition from p-type to n-type, and back to p-type, leaves no doubt that p-type ZnO does exist, and also provides a reasonable explanation of why p-type ZnO sometimes seems unstable. We should further note that more strongly p-type ZnO, such as that illustrated in figure 5, does not become n-type even under strong light.

Background donors and acceptors in ZnO

Until recently, most reports involving n-type ZnO have attributed the dominant donor to either the oxygen vacancy V_O or the Zn interstitial Zn_i . However, it is now known that V_O is not shallow but deep, and that both V_O and Zn_i have high equilibrium formation energies in n-type ZnO. It is still possible that Zn_i could be important in certain non-equilibrium situations, but most researchers now believe that the dominant background donors are H and the group III elements Al and Ga.

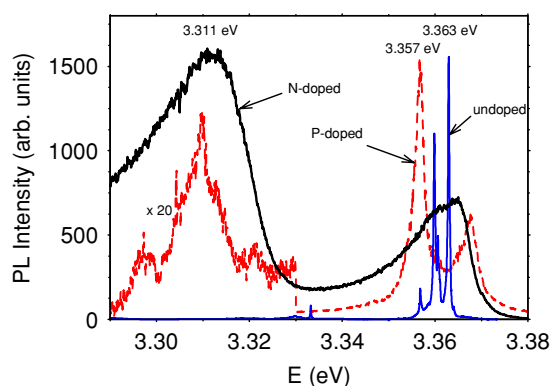


Figure 6. Photoluminescence spectra at 4 K for bulk, undoped ZnO grown from the vapour phase (solid line), N-doped ZnO grown by MBE (chained line), and P-doped ZnO grown by rf sputtering (dashed line).

Several recent experiments have confirmed the existence of H in ZnO, at an energy of 30–40 meV [38–41]. Bulk ZnO, grown by a vapour-phase method, typically displays two donors, a shallower one at 30–40 meV, and a deeper one at 60–70 meV [34], as shown in figure 2. From annealing experiments, we believe that the shallower donor is H, and that this donor also has a photoluminescence (PL) signature, a donor-bound exciton transition at 3.363 eV, as shown in figure 6. However, besides the 31 meV donor in figure 2, there also is a 61 meV donor of significantly higher concentration. Perhaps the best candidate for this somewhat deeper donor is Al_{Zn} [42], since it is known that Al is a contaminant in ZnO, and that deliberate Al doping can produce very high free electron concentrations [43].

We now turn to the background *acceptors*. The undoped, bulk sample represented by figures 1 and 2, and by the

spectrum with the sharpest PL lines in figure 6, has been shown by temperature-dependent Hall-effect measurements to have an acceptor concentration of only $2 \times 10^{15} \text{ cm}^{-3}$ as mentioned above. Recent positron annihilation measurements on this same material identify this acceptor as the Zn vacancy, V_{Zn} [44]. Theory also finds that V_{Zn} should have a relatively low formation energy in n-type ZnO [45, 46]. Of course, other types of crystal growth can lead to other types of acceptors and donors; thus, research on these matters must continue.

Acceptor dopants in ZnO

As seen in table 1, many different growth techniques and acceptor species have been used for the successful growth of p-type ZnO. (Table 1 is a summary of pertinent information on p-type ZnO samples reported in the literature, and is a modified and updated version of a table presented earlier [31].) The first report of hole conduction in ZnO, by Minegishi *et al* [4], was based on N doping. Indeed, as seen in table 1, most of the attempts to produce p-type ZnO have employed N as the acceptor of choice. Other acceptor dopants, besides N, have also been explored. The most obvious choices are perhaps the other group V elements, P and As, which also might be expected to substitute for O. However, density functional theory (DFT) predicts that P_{O} should have an acceptor level at 0.93 eV, as compared to 0.40 eV predicted for N_{O} [47]. The reason for the large difference in these energies is the ionic size mismatch between P and O. Nevertheless, in spite of the theoretical discouragement, Aoki *et al* [48] have used laser doping of P (from Zn_3P_2) to produce a homojunction diode exhibiting light emission, implying that p-type ZnO was formed. Then more recently, Kim *et al* [19] have used P_2O_5 to produce excellent p-type material, with a resistivity of only

Table 1. Data on p-type ZnO samples reported in the literature.

First author	Technique	Dopant	Resistivity ($\Omega \text{ cm}$)	Year of publication	Reference
Minegishi	CVD	N	34	1997	4
Joseph	PLD	N	4	1999	5
Ryu	PLD	As	?	2000	6
Joseph	PLD	N, Ga	0.5	2001	7
Guo	PLD	N	2	2001, 2002	8
Butkhuzi	Quasi-epi	none	900	2001	9
Ashrafi	MOMBE	N	?	2002	10
Xiong	DC mag. sputt.	none	3	2002	11
Look	MBE	N	40	2002	12
X Li	MOCVD	N	20	2003	13
Bang	RF mag. sputt.	P	?	2003	14
B S Li	CVD	N	150	2003	15
Singh	RF diode sputt.	N, Ga	12	2003	16
Huang	DC mag. sputt.	N	1	2003	17
Ryu	Hybrid beam	As	2	2003	18
Kim	RF sputt.	P	0.6	2003	19
Lu	DC mag. sputt.	N	31	2003	20
J Wang	MOCVD	N	100	2003	21
C Wang	DC mag. sputt.	N	83	2003	22
Rommelueire	MOVPE/diffusion	N	0.6	2003	23
Lu	CVD	N	20	2003	24
Ma	MOVPE	none	43	2004	25
Lin	RF mag. sputt.	N	10	2004	26
Ye	DC mag. sputt.	N, Al	160	2004	27
Xu	MOCVD	N	3	2004	28
Look	Evaporation/sputt.	As	0.4	2004	29

0.6 Ω cm. Thus, either DFT is inaccurate in this case, or the acceptor is not simple substitutional P_O . In this regard, new acceptor defect structures involving P are now being proposed. One complication with P doping is that a donor state, perhaps involving P_{Zn} instead of P_O , is also evidently possible, and may be a source of concern [49].

If P_O is predicted to be deep, then As_O should be even deeper, and indeed DFT finds an acceptor level of 1.15 eV for this impurity. On the other hand, Ryu *et al* have grown As-doped ZnO layers on Al_2O_3 , and have found them to be p-type, with an activation energy of about 120 meV [18]. Finally, Renlund *et al* [29] have used evaporation of Zn_3As_2 and subsequent sputtering of ZnO to produce As-doped ZnO, some of which is illustrated in figure 5. The solid line through the mobility is derived from the theory presented earlier, with the valence band modelled simply as a single band with an effective mass of $0.64m_0$. The fitting parameters are then: $N_A = 9 \times 10^{19} \text{ cm}^{-3}$ and $N_D = 8 \times 10^{19} \text{ cm}^{-3}$, illustrating that a very high concentration of As has been incorporated. SIMS measurements agree, giving an As concentration in the mid- 10^{19} cm^{-3} range.

The successes in producing p-type ZnO with P and As are somewhat unexpected, as mentioned earlier. One theoretical suggestion is that As does not enter the lattice simply as As_O , but as $As_{Zn}-2V_{Zn}$ [50]. Calculations indicate that the latter defect complex should have an acceptor level at about 150 meV, shallower than that of As_O , and should also have a lower formation energy than that of As_O . A similar scenario evidently also applies to Sb as an acceptor dopant. These interesting possibilities must be subject to verification, and relevant experiments are already underway.

Group I elements, substituting on the Zn site, are also acceptor candidates. Li, Na and K, are predicted to have acceptor energy levels of 0.09, 0.17 and 0.32 eV, respectively [47]. These levels are shallower than those predicted for N_O , P_O and As_O . However, it is well known that Li doping actually produces semi-insulating (SI) ZnO [12], and the reason likely involves formation of the Li interstitial Li_I , which has a donor nature [47]. That is, as the Fermi level E_F drops due to the formation of Li_{Zn} acceptor centres, it will become more and more favourable for Li_I donors to form, and eventually E_F will settle at an energy between the donor and acceptor levels, i.e., near midgap. The same mechanism should hold for Na doping. For K doping, on the other hand, it will probably be the formation of V_O donors that will keep the sample from transforming to p-type [47]. If the theoretical considerations are valid, then group-I dopants may be useful only for producing SI ZnO, not p-type ZnO.

Photoluminescence fingerprints of acceptors

In figure 6, we compare the PL spectrum of N-doped ZnO, grown by MBE on a Li-doped, SI ZnO substrate, with that of bulk, undoped ZnO. Besides the much broader D^0X lines near 3.36 eV, probably due to the high concentration of N ($>10^{19} \text{ cm}^{-3}$), a new, strong line appears at 3.315 eV [12]. Other groups have seen similar lines in N-doped ZnO [15, 20, 51]. In [12], it was suggested that this line represents an acceptor-bound exciton (A^0X), and in this same reference, the N_O acceptor energy was estimated, from the optical data,

to be in the range 170–200 meV. In agreement, Zeuner *et al* [52] have suggested an optical energy of 165 ± 40 meV for N_O . More recently, from Hall-effect measurements, we have found an energy of about 90 meV, as derived from the slope of the line in figure 3 [30]. It is perhaps not too surprising that the Hall activation energy is lower than the optical energy, because this is nearly always the case, due to screening. If the free-exciton energy is 3.377 eV, then the binding energy to the N_O acceptor is 62 meV, which implies a Haynes factor of about $62/200 = 0.31$, a rather large value. Because of this difficulty, some authors have suggested that the 3.315 eV line is a donor–acceptor pair (D^0-A^0) transition [20, 51], rather than an A^0X transition. But the D^0-A^0 assignment also is controversial, because (1) the line does not blue-shift with laser excitation intensity [15], and (2) an energy of 3.315 eV would imply an acceptor energy of <100 meV. (The latter relationship results from the fact that $E_{D-A} = E_g - E_D - E_A + \langle e^2/4\pi\epsilon r \rangle = 3.437 - 0.06 - E_A + 0.02$, implying that $E_A \approx 80$ meV.) Such a small value from an optical measurement of E_A is unlikely, considering that all of the measurements or estimates in the literature so far suggest that the optical E_A for N_O is well above 100 meV. Again, at this stage, the origin of the 3.315 eV line is not clear, and further research will be necessary.

P-doped ZnO also displays a transition near 3.31 eV, as shown in figure 6. Thus, this transition, whatever its origin, seems to be associated with relatively shallow acceptors. Also, note that the well-known 3.357 eV line is greatly enhanced in both the N-doped and P-doped samples, especially the latter. This transition has been assigned to both an acceptor-bound exciton [53], and a donor-bound exciton [54].

Summary

The quest to produce p-type ZnO is now a reality, but detailed knowledge of its electrical and optical properties is still lacking. The most common acceptor dopant is N_O , and its energy level has been reported to be about 135 meV, from electrical measurements, and 150–210 meV, from photoluminescence data. Also, doping with P, As and Sb, produces p-type material, but the detailed lattice structures of these elements, as acceptors, are not known. For most of the p-type samples studied so far, the photoluminescence results yield a prominent line near 3.31 eV, and also seem to emphasize the well-known donor-bound exciton lines at 3.357 and 3.367 eV.

Acknowledgments

The support of US Air Force Contract F33615-00-C-5402 is gratefully acknowledged. Also, thanks are due to B Claflin, C W Litton, D C Reynolds, G Cantwell, G M Renlund and S J Park for helpful discussions.

References

- [1] Nishi J *et al* 2003 *Japan. J. Appl. Phys.* **42** L347
- [2] Shibata N, Uemura T, Yamaguchi H and Yasukawa T 2003 *Phys. Status Solidi a* **200** 58
- [3] Look D C 2001 *Mater. Sci. Eng. B* **80** 383
- [4] Minegishi K, Koiwai Y and Kikuchi K 1997 *Japan. J. Appl. Phys.* **36** L1453

- [5] Joseph M, Tabata H and Kawai T 1999 *Japan. J. Appl. Phys.* **38** L1205
- [6] Ryu Y R, Zhu S, Look D C, Wrobel J M, Jeong H M and White H W 2000 *J. Cryst. Growth* **216** 330
- [7] Joseph M, Tabata H, Saeki H, Ueda K and Kawai T 2001 *Physica B* **302–303** 140
- [8] Guo X-L, Tabata H and Kawai T 2001 *J. Cryst. Growth* **223** 135
Guo X-L, Tabata H and Kawai T 2002 *Opt. Mater.* **19** 229
- [9] Butkhuzi T V, Sharvashidze M M, Gamkrelidze N M, Gelovani Kh V, Khulordava T G, Kekelidze N P and Kekelidze E E 2001 *Semicond. Sci. Technol.* **16** 575
- [10] Ashrafi A B M A, Suemune I, Kumano H and Tanaka S 2002 *Japan. J. Appl. Phys.* **41** L1281
- [11] Xiong G, Wilkinson J, Mischuck B, Tuzemen S, Ucer K B and Williams R T 2002 *Appl. Phys. Lett.* **80** 1195
- [12] Look D C, Reynolds D C, Litton C W, Jones R L, Eason D B and Cantwell G 2002 *Appl. Phys. Lett.* **81** 1830
- [13] Li X, Yan Y, Gessert T A, Perkins C L, Young D, DeHart C, Young M and Coutts T J 2003 *J. Vac. Sci. Technol. A* **21** 1342
Li X, Yan Y, Gessert T A, DeHart C, Perkins C L, Young D and Coutts T J 2003 *Electrochem. Solid-State Lett.* **6** C56
- [14] Bang K H, Hwang D-K, Park M-C, Ko Y-D, Yun I and Myoung J-M 2003 *Appl. Surf. Sci.* **210** 177
- [15] Li B S, Liu Y C, Zhi Z Z, Shen D Z, Lu Y M, Zhang J Y, Fan X W, Mu R X and Henderson D O 2003 *J. Mater. Res.* **18** 8
- [16] Singh A V, Mehra R M, Wakahara A and Yoshida A 2003 *J. Appl. Phys.* **93** 396
- [17] Huang J, Ye Z, Chen H, Zhao B and Wang L 2003 *J. Mater. Sci. Lett.* **22** 249
- [18] Ryu Y R, Lee T S and White H W 2003 *Appl. Phys. Lett.* **83** 87
- [19] Kim K-K, Kim H-S, Hwang D-K, Lim J-H and Park S-J 2003 *Appl. Phys. Lett.* **83** 63
- [20] Lu J, Zhang Y, Ye Z, Wang L, Zhao B and Huang J 2003 *Mater. Lett.* **57** 3311
- [21] Wang J *et al* 2003 *J. Cryst. Growth* **255** 293
- [22] Wang C, Ji Z, Liu K, Xiang Y and Ye Z 2003 *J. Cryst. Growth* **259** 279
- [23] Rommeluère J F, Svob L, Jomard F, Mimila-Arroyo J, Lusson A, Sallet V and Marfaing Y 2003 *Appl. Phys. Lett.* **83** 287
- [24] Lu J-G, Ye Z-Z, Wang L, Huang J-Y and Zhao B-H 2003 *Mater. Sci. Semicond. Process.* **5** 491
- [25] Ma Y, Du G T, Yang S R, Li Z T, Zhao B J, Yang X T, Yang T P, Zhang Y T and Liu D L 2004 *J. Appl. Phys.* **95** 6268
- [26] Lin C-C, Chen S-Y, Cheng S-Y and Lee H-Y 2004 *Appl. Phys. Lett.* **84** 5040
- [27] Ye Z-Z, Ge F-Z, Lu J-G, Zhang Z-H, Zhu L-P, Zhao B-H and Huang J-Y 2004 *J. Cryst. Growth* **265** 127
- [28] Xu W-Z, Ye Z-Z, Zhou T, Zhao B-H, Zhu L-P and Huang J-Y 2004 *J. Cryst. Growth* **265** 133
- [29] Look D C, Renlund G M, Burgener R H II and Sizelove J R *Appl. Phys. Lett.* at press
- [30] Look D C and Claffin B 2004 *Phys. Status Solidi b* **241** 624
- [31] Look D C, Claffin B, Ya I Alivov and Park S J 2004 *Phys. Status Solidi a* **201** 2203
- [32] Look D C 1989 *Electrical Characterization of GaAs Materials and Devices* (New York: Wiley) chapter 1
- [33] Look D C and Sizelove J R 1999 *Phys. Rev. Lett.* **82** 1237
- [34] Look D C, Reynolds D C, Sizelove J R, Jones R L, Litton C W, Cantwell G and Harsch W C 1998 *Solid State Commun.* **105** 399
- [35] Heo Y W, Kwon Y W, Li Y, Pearson S J and Norton D P 2004 *Appl. Phys. Lett.* **84** 3474
- [36] Kim S, Kang B S, Ren F, Heo Y W, Ip K, Norton D P and Pearson S J 2004 *Appl. Phys. Lett.* **84** 1904
- [37] Claffin B *et al* 2004 unpublished
- [38] Hofmann D M, Hofstaetter A, Leiter F, Zhou H, Henecker F, Meyer B K, Orlinskii S B, Schmidt J and Baranov P G 2002 *Phys. Rev. Lett.* **88** 5504
- [39] Look D C, Jones R L, Sizelove J R, Garces N Y, Giles N C and Halliburton L E 2003 *Phys. Status Solidi a* **195** 171
- [40] Strzhemechny Y M, Nemergut J, Smith P E, Bae J, Look D C and Brillson L J 2003 *J. Appl. Phys.* **94** 4256
- [41] Seager C H and Myers S M 2003 *J. Appl. Phys.* **94** 2888
- [42] Shibata H *et al* 2004 *Phys. Status Solidi c* **1** 872
- [43] Makino T, Segawa Y, Yoshida S, Tsukazaki A, Ohtomo A and Kawasaki M 2004 *Appl. Phys. Lett.* **85** 759
- [44] Tuomisto F, Saarinen K and Look D C 2003 *Phys. Rev. Lett.* **91** 205502
- [45] Zhang S B, Wei S H and Zunger A 2001 *Phys. Rev. B* **63** 075205
- [46] Kohan A F, Ceder G, Morgan D and Van de Walle C G 2000 *Phys. Rev. B* **61** 15019
- [47] Park C H, Zhang S B and Wei S H 2002 *Phys. Rev. B* **66** 073202
- [48] Aoki T, Hatanaka Y and Look D C 2000 *Appl. Phys. Lett.* **76** 3257
- [49] Heo Y W, Park S J, Ip K, Pearson S J and Norton D P 2003 *Appl. Phys. Lett.* **83** 1128
- [50] Limpitjumnong S, Zhang S B, Wei S-H and Park C H 2004 *Phys. Rev. Lett.* **92** 155504
- [51] Nakahara K, Takasu H, Fons P, Yamada A, Iwata K, Matsubara K, Hunger R and Niki S 2001 *Appl. Phys. Lett.* **79** 4139
- [52] Zuener A, Alves H, Hofmann D M, Meyer B K, Hoffmann A, Haboeck U, Strassburg M and Dworzak M 2002 *Phys. Status Solidi b* **234** R7
- [53] Gutowski J, Presser N and Broser I 1988 *Phys. Rev. B* **38** 9746
- [54] Strassburg M *et al* 2004 *Phys. Status Solidi b* **241** 607